

## Visible and Infrared Photoinjection of Electrons into Insulating Layers of MIS Memory Devices.

Y. Komiya, T. Sakamoto, E. Suzuki and Y. Tarui

Electrotechnical Laboratory  
Tanashi, Tokyo

Photoinjection in MIS device is of current interest because of investigation for behavior of hot carrier injections<sup>(1), (2)</sup> in non-volatile memory action and applications<sup>(2)</sup> to optical input pattern memory. Hitherto, photoinjection of carriers into insulating layers of MIS device have been limited in the high energy wave length region such as ultraviolet light.<sup>(1), (2)</sup>

In this paper, visible and infrared photoinjection of electrons into MIS device have been experimentally verified and theoretically investigated by means of illuminating monochromatic light on a relatively high field depletion region of the substrate, where the field is not sufficient to produce avalanche injection. In Fig.1 are shown the incident photon flux and the direct gate current in a semitransparent gate Au film (~200Å)-SiO<sub>2</sub>(1100 Å)-Si diode which flows when the MIS capacitor is driven by a large amplitude R.F. signal (100KHz~1 MHz) as shown in Fig.3 under visible and infrared monochromatic light exposure. Photoinjection efficiencies of gate currents per unit photon flux calculated from Fig.1 are shown in Fig.2 as a function of photon wave lengths.

In order to explain the fundamental characteristics of photon enhanced ionization injection of hot carriers into MIS gate, a physical model as illustrated in Fig.4 is assumed.

The theoretical treatment of ionization process under a high field is almost the same as the previous paper by J.L.Moll et al<sup>(3)</sup>, but it is modified to introduce photon enhanced ionization as follows.

$\mathcal{E}_r$  = optical phonon energy = 0.063 eV ,  $\mathcal{E}_i$  = ionization threshold = 2.08 eV ,  
 $l_r$  = mean free path for optical phonon scattering<sup>(4)</sup> = 60 Å ,  
 $l_i$  = mean free path for ionization<sup>(4)</sup> = 190 Å ,  $\alpha_i(x)$  = ionizations / cm ,  
 $\alpha_r$  = optical phonon emission / cm ,  $\alpha_{ro}$  = optical phonon collisions that occur at low energy ( number of cold starts ) ,  $\alpha_{rh}$  = optical phonon emission that occur at high carrier energies larger than  $\mathcal{E}_i$  ,  $P(E)$  = probability that either a single or multiple stage ionization occurs ( per cold start )

$$P(E) = \exp(-\mathcal{E}_i/qEl_r) / \left\{ (1+r) \left( 1 - \frac{r}{1+r} \exp(-\mathcal{E}_r/qEl) \right) \right\} , \quad l^{-1} = l_i^{-1} + l_r^{-1}$$

$$\alpha_i = P(E) \alpha_{ro} , \quad \alpha_{rh} = r \alpha_i = r P(E) \alpha_{ro} , \quad r = l_i / l_r$$

The number of cold start electron is assumed to be proportional to the local photon adsorption ( $\Phi \alpha e^{-\alpha x}$ )

$$\alpha_{ro} = K \Phi \alpha e^{-\alpha x} , \quad \alpha(\lambda) = \text{adsorption coefficient at } \lambda , \quad \Phi = \text{flux density of photon,}$$

$$\alpha_i(x) = P(E) \cdot K \Phi \alpha e^{-\alpha x}$$

Assuming the depletion region of MIS capacitor as same as that of N<sup>+</sup>P step junction , the total multiplied electron current  $I_n(0)$  at  $x = 0$  and the injected gate current are given as a function of  $\lambda$ , followingly.

$$I_n(0) = M_n \cdot I_n(W) , \quad I_n(W) = \frac{qD_n}{L_n} \Phi \alpha \exp(-\alpha W) , \quad \alpha_n(x) = P(E) \cdot K \Phi \alpha e^{-\alpha x}$$

$$1 - \frac{1}{M_n} = \int_0^W \alpha_n \exp\left[-\int_0^x (\alpha_n - \alpha_p) dx'\right] dx = \frac{1}{1-r} \left[ 1 - \exp\left(-\int_0^W \alpha_n dx\right) - (1-r) \alpha_n dx \right]$$

$$\alpha_p = \gamma \alpha_n , \quad I_G(\lambda) = I_n(0, \lambda) \exp(-E_b^i / kT_e)$$

In Fig.2, a theoretical computer calculation of  $I_G(\lambda)$  as a function of  $\lambda$  is fitted with the experimental one. The maximum injection rate is observed at  $\lambda_m = 0.54 \mu$ . The injection rate decreases at the shorter wave lengths than  $\lambda_m$ , because adsorption mainly occurs at the low potential region near the interface. On the other hand, the injection rates decreases at the longer wavelength than  $\lambda_m$  because the longer wave lights are not completely adsorbed in the high field depletion region.

Photoinjection of hot carriers in case of a semitransparent Au gate MOS transistor ( $t_{ox} = 1100 \text{ \AA}$ ,  $l_{ch} = 6.15 \mu$ ) and  $10 \times 10$  MAOS transistor matrix ( $t_{ox} = 1100 \text{ \AA}$ ,  $1500 \text{ \AA}$ ,  $t(\text{Al}_2\text{O}_3) = 2700 \text{ \AA}$ ,  $l_{ch} = 15 \mu$ ) have also been examined at visible and infrared region. Preliminary experiments by MAOS transistors suggest that electron injections are observed in case of a large R.F. signal +DC bias such as T(2) mode shown in Fig.5 and positively charged traps after photoinjection is observed in case of a large R.F. signal such as T(1) mode in Fig.5.

We are grateful to Dr. Y. Komamiya for his encouragement and to H. Teshima, Y. Hayashi, T. Koyanagi for their cooperation and to N. Tsujimoto and N. Uchida for their cooperation for experiment.

- (1) C.N. Berglund and R.J. Powell : J. Appl. phys. vol.42, No.2 p573, 1971
- (2) Y. Tarui et al : Proc. 4th Conf. on Sol. St. Devices, Tokyo, 5-1, 1972
- (3) J.L. Moll : Physics of Semiconductors, McGraw Hill, p216 1964
- (4) D.J. Bartelink et al : Phys. Rev. Vol.130, No.3, p972, 1963

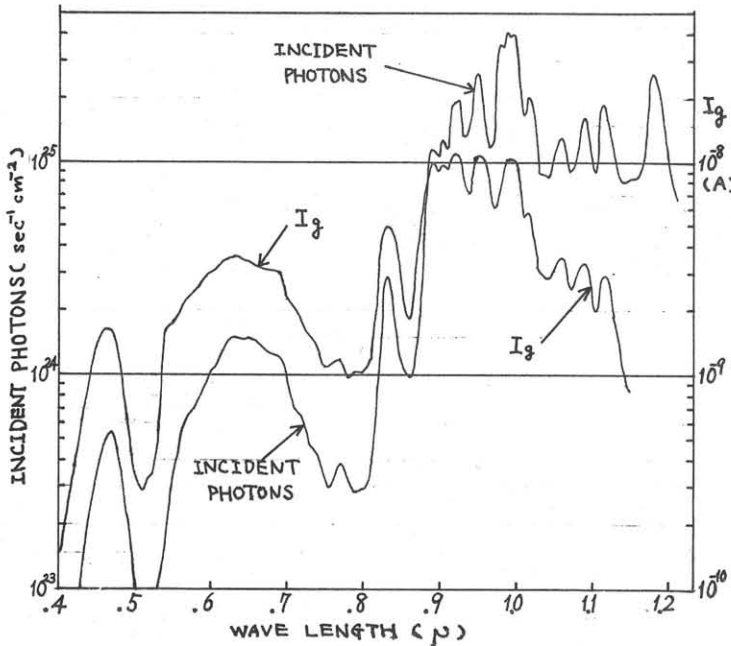


Fig.1 The incident photon flux and the photoinjected direct gate current vs. photon wavelength.

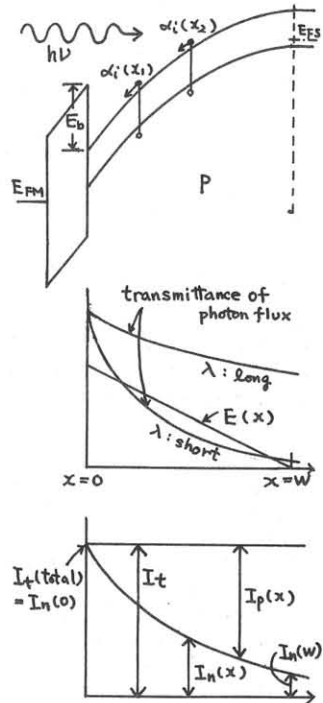


Fig.4 Band diagram and physical model for photoinjection

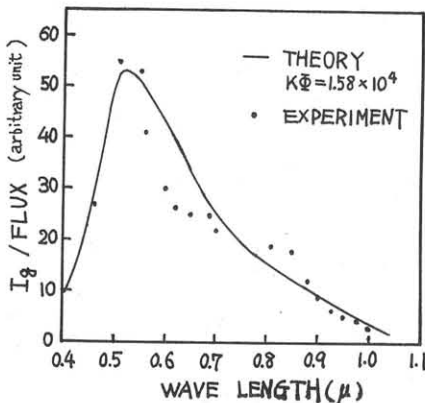


Fig.2 Photoinjection efficiencies of gate currents per unit photon flux vs. photon wavelength

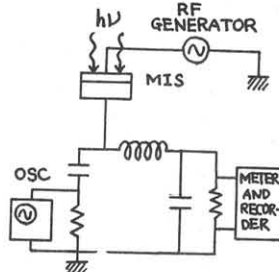


Fig.3 Measuring circuit for photoinjection.

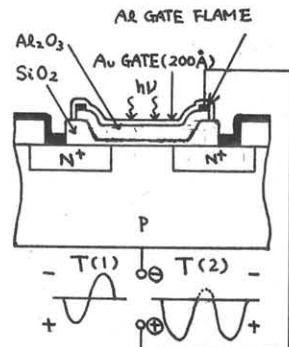


Fig.5 Operation mode of MAOS transistor for visible and infrared photoinjection.